

Punicalagin induces ROS-mediated apoptotic cell death through inhibiting STAT3 translocation in lung cancer A549 cells

Le Fang^{1,2} | Hong Wang³  | Jie Zhang⁴ | Xiaolei Fang⁴ 

¹Department of Clinical Laboratory, The 521 Hospital of Ordnance Industry, Xi'an, Shaanxi, China

²Department of Blood Transfusion, Institute for Hygiene of Ordnance Industry, Xian, Shaanxi, China

³Laboratory of Toxicology and Biological Effect, Institute for Hygiene of Ordnance Industry, Xian, Shaanxi, China

⁴Department of Blood Transfusion, Ankang City Central Hospital, Ankang, Shaanxi, China

Correspondence

Xiaolei Fang, Department of Blood Transfusion, Ankang City Central Hospital, 725000 Ankang, Shaanxi 725000, China.
Email: fangxl1120@sina.com

Funding information

Natural Science Basic Research Plan in Shaanxi provenance of China, Grant/Award Number: 2019JQ-993

Abstract

Lung cancer is a noxious disease with substandard overall survival. Despite this, there are several treatment strategies for lung cancer include chemotherapy, radiotherapy, surgery; however, the overall survival remains poor. Punicalagin has been documented as a potential phytomedicine to selectively inhibit the progression and expansion of numerous cancers. In the present study, we evaluated the antiproliferative ability of punicalagin against lung cancer A549 cells by inducing apoptosis by inhibiting STAT-3 activation. Punicalagin induces toxic effects of A549 cells in a dose-associated manner after 24 h treatment. And we also observed that punicalagin (10, 20, and 30 μ M) induced reactive oxygen species generation, alters the mitochondrion membrane potential and apoptotic morphological changes in A549 cells. The STAT-3 overexpression regulates apoptosis, proliferation, and angiogenesis. Here, the punicalagin inhibited STAT-3 translocation and thereby induces apoptosis by inhibiting expression Bcl-2 and enhanced expression of Bax, cytochrome-c, caspase-9, and caspase-3 in A549 cells. Hence, we stated that the punicalagin is a possible therapy for non-small cell lung, malignancies. Altogether, the punicalagin is a promising phytomedicine in malignancy treatment and further endeavors are needed to unveil the complete potential.

KEYWORDS

apoptosis, lung cancer, phytodrug, punicalagin, STAT-3

1 | INTRODUCTION

Lung malignant growth is the chief reason for disease-related mortality and it is responsible for 1/5 of all malignant mortality.^[1] More than 1.8 million new patients have been diagnosed and 1.6 million deadly cases have been recorded so far each year. Around 85%–90% of all lung cancer patients have non-small cell lung disease.^[2] At the present time, the most commonly available treatments are surgical removal, radiotherapy, and chemotherapy. Despite this, the recuperating effect is not adequate and the 5-year survival rate for lung malignancy is 15% only. Thus, it is important to search for a novel and better therapy for

lung malignant growth.^[3] For the past couple of decades, numerous FDA-approved inhibitors for epidermal growth factor receptor (EGFR)-directed tyrosine kinase inhibitors (TKIs) have been established such as afatinib, erlotinib, and gefitinib for non-small cell lung cancer (NSCLC) treatment.^[4] However, the essential productivity and the expansion of subordinate drug resistance has become the chief limitation for these drugs.

Cisplatin, doxorubicin, paclitaxel, and so forth, are high potential anticancer drugs that are extensively used to manage different human malignancies such as bladder, breast, and multiple myeloma.^[5] However, these types of drugs are extremely toxicity producing and have unusual

side effects. Hence, it is important to find new strategies to improve chemotherapeutics by using photochemical-based treatment strategies against NSCLC. As malignant cells contain elevated amounts of reactive oxygen species (ROS) when compared with ordinary cells, this results in cell survival and multiplication.^[6] The extreme production of ROS creates cellular homeostasis that leads to cell injury. At a lesser level of ROS, cells involve in several biological processes like survival of cancer cells, differentiation, and gene expansion or proliferation. As in higher levels, it exerts oxidation-mediated stress, which leads to cell death via various molecular signaling pathways.^[7,8] The modern research revealed that the predominant genotype-based targeted therapies for NSCLC are transcription factor inhibition-based approaches. The unusual expression of signal transducer and activator of transcription-3 (STAT-3) cause tumor development, metastasis and drug resistance in different human cancers, including NSCLC.^[9] This means that the STAT3 gets resistant toward existing therapy of NSCLC. STAT3 signaling has been considered as a major intrinsic pathway involved in the induction of cancer and inflammation. Moreover, it can regulate several genes such as cell proliferative and apoptotic markers.^[10] Phosphorylation of STAT-3 is translocated into the nucleus and it activates cell proliferation and diminishes the apoptotic pathway via upregulation of Bcl-2 proteins.^[11] Therefore, inhibition of STAT-3 molecules has been considered a novel target for inducing apoptosis.

Recently, an enormous number of natural molecules have been recognized as having an efficient antitumor activity.^[12] Increasing evidence postulated that the Pomegranate (*Punica granatum*), a notable ancient natural product possess potential chemopreventive molecules that prevents several kinds of cancer.^[13,14] Punicalagin is the chief bioactive component in the pomegranate peel, and has anti-inflammatory, antioxidant, antiproliferation, antiviral, and anticancer properties.^[15,16] Also, in different tumor cell lines, previous reports found that the punicalagin upregulates the articulation levels of Bax, Bcl-2, and cytochrome c; induction of caspase-3 and caspase-9 expression thereby modulates proliferation and apoptosis.^[17] Janus kinase-1 (JAK-1) is of concern as a member of tyrosine kinases, which is bound with the cytoplasmic areas of cytokine receptors especially interleukin-6 (IL-6). The multimerization of IL-6 receptors can initiate or activate the JAK transphosphorylation that subsequently activates the STAT-3 translocation through the phosphorylation process.^[18] Therefore, in this study, we have evaluated inhibiting punicalagin-induced lung cancer A549 cell proliferation by JAK-1-mediated STAT-3 translocation.

2 | MATERIALS AND METHODS

2.1 | Reagents and antibodies

Punicalagin ($\geq 98\%$ HPLC), 3-(4,5-dimethyl-2-thiazolyl)-2,5-diphenyltetrazolium bromide (MTT), acridine orange, 2'-7'-dichlorofluorescein diacetate (DCFH-DA), Rhodamine-123, Hoechst were obtained from the chemical supplier, Sigma-Aldrich. The cell

culture, chemicals which are EDTA, Dulbecco's modified Eagle's medium (DMEM) medium, penicillin-streptomycin, fetal bovine serum (heat-inactivated FBS), phosphate-buffered saline (PBS), and glutamine were acquired from Cell Signaling Technology. The antibodies (BAX, STAT-3, caspase-3, cytochrome-c, caspase-9, IL-6, Bcl-2, JAK-1) were supplied from Santa Cruz Biotechnology.

2.2 | Cell culture and treatments

The lung cancer cell A549 and normal human dermal fibroblast (HDF) cells were procured from the American Type Culture (ATC). Both A549 and HDF cells were cultured with the addition of DMEM along with 1% penicillin/streptomycin and 10% FBS. Moreover, cells were placed incubated with a distribution of 5% CO₂ gas, which maintains the humidity and 37°C temperature. The growth of the cells was monitored by an inverted microscope. After reaching the appropriate confluency of A549, the cells were treated with punicalagin in three different concentrations (10, 20, and 30 μM) for 24 h incubation. Then, the cells were scraped to allow for experiments. The purity of punicalagin was shown as $\geq 98\%$ HPLC grade and it was dissolved in molecular grade double-distilled water.

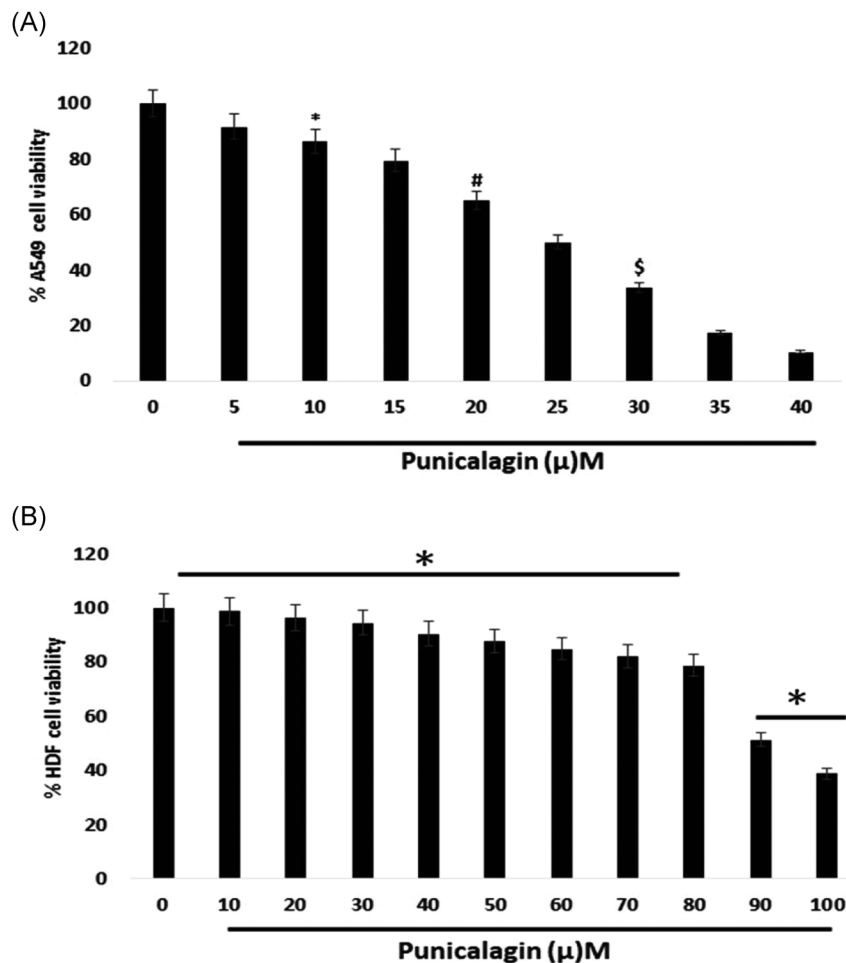
2.3 | MTT assay

The cellular toxic nature of punicalagin was assessed by MTT-based calorimetric test.^[19] The A549 and HDF cells were equally distributed (5000 cells/well) in 96-well plates and then incubated for 24 h at 37°C in CO₂ nature. Next, various concentrations of punicalagin were exposed to the cells to examine toxicity. Then, the cells were incubated for 24 h. Then, yellow MTT reagent was exposed to the treated and control cells; following that they were kept incubated around 4–6 h at 37°C. Then, the medium along with MTT solution was removed and 100 μl of dimethyl sulfoxide was mixed into the well, breaking down the crystal purple formazan and the absorbance was calculated at 570 nm by using a microplate reader.

2.4 | ROS determination

Punicalagin treatment associated ROS generation could be analyzed by A549 cells stained with a DCFH-DA probe followed by spectrofluorimetric estimation.^[20] Lung carcinoma A549 cells were distributed uniformly on the six numbered well plates; after 24 h, punicalagin was exposed to the medium and treated to cells following incubation on CO₂ for 24 h. Thereafter, the A549 cells could be allowed to stain by a DCFH-DA fluorescent probe for 30 min incubation. Finally, the intensity of the fluorescence was estimated by excitation (485 ± 10) and emission (530 ± 12.5 nm) channels, respectively. In addition, levels of punicalagin-induced quantification of ROS were determined by flow cytometry (BD Biosciences).

FIGURE 1 Punicalagin produces toxicity against A549 cells and is nontoxic against HDF cells. (A) The toxic role of punicalagin against A549 cells calculated by MTT assay. (B) The nontoxic concentration of punicalagin against HDF cells was evaluated by MTT assay. Values from the statistical data are articulated as mean \pm SD for three separate experiments. Values not allocated a marking (*, #, \$) vary significantly at $p < 0.05$ versus control (DMRT). DMRT, Duncan's multiple range test; HDF, human dermal fibroblasts; MTT, 3-(4,5-dimethyl-2-thiazolyl)-2,5-diphenyltetrazolium bromide



2.5 | Rhodamine 123 staining

The potential alteration of the mitochondrial membrane was assessed by the method of Rhodamine-123 fluorescent probe staining.^[21]

TABLE 1 Shows the punicalagin-mediated % cell viability in A549 cells

| Punicalagin (μM) | Average Mean | % Cell viability | SD |
|------------------|--------------|------------------|----------|
| 0 | 5.187 | 100 | 0.10374 |
| 5 | 4.743667 | 91.45299 | 0.094873 |
| 10 | 4.089667 | 86.2132 | 0.081793 |
| 15 | 3.245333 | 79.35447 | 0.064907 |
| 20 | 2.111 | 65.04725 | 0.04222 |
| 25 | 1.056 | 50.02369 | 0.02112 |
| 30 | 0.353333 | 33.4596 | 0.007067 |
| 35 | 0.061 | 17.26415 | 0.00122 |
| 40 | 0.006333 | 10.38251 | 0.000127 |

2.6 | Acridine orange and ethidium bromide (AO/EB) staining

Fluorescence microscopic examination of apoptotic cell death was assessed by the AO/EB twofold staining method; studying the apoptotic detection via morphological examination.^[22]

2.7 | Hoechst staining

The nuclear fragments were detected by Hoechst staining with microscopic examination. Approximately, A456 cells (1×10^5) were uniformly distributed in six numbered well plates and exposed to punicalagin (24 h). Next, the cells could be probed with Hoechst for 30 min. The bright stained fragmented cells were examined by a fluorescent microscope with a blue filter channel.^[23]

2.8 | Western blot analysis

The different concentrations of punicalagin (10, 20, and 30 μM) were treated with A549 cells and incubated for 24 h. Then, the

cells were rinsed properly by using phosphate buffered saline (PBS) and whole extracts were collected in a radio-immunoprecipitation assay lysis buffer including 1% β -mercaptoethanol and protease inhibitor cocktail and then allowed to centrifuge highly (13,000g for 15 min). Moreover, the cytosolic and nuclear fractions were collected by using a suitable buffer. Briefly, the cell pellets were suspended in cytosolic buffer solution (1.5 mM $MgCl_2$, 10 mM HEPES, 10 mM KCl, pH 7.9, 0.1 mM EDTA, 1 mM 2'-7'-dichlorofluorescein diacetate (DCF),

0.1 mM EGTA, aprotinin, 0.5 mM phenylmethylsulfonyl fluoride (PMSF), leupeptin, 1 mM Na_3VO_4 , 1 mmol·L⁻¹ NaF) for 15 min at ice tray. Then, the A549 cells were fully lysed with 10% nonidet P-40. Then, allowed again high centrifugation (13,000g for 5 min), the collected supernatant was used as a cytosolic extract. Similarly, for nuclear extract preparation after treatment, A549 cells were suspended in nuclear buffer (400 mM NaCl, 20 mM HEPES, 1 mM EDTA, pH 7.9, 1 mM DTT, 1 mM EGTA, 1 mM PMSF, leupeptin and aprotinin) on ice tray for 15 min. Then finally

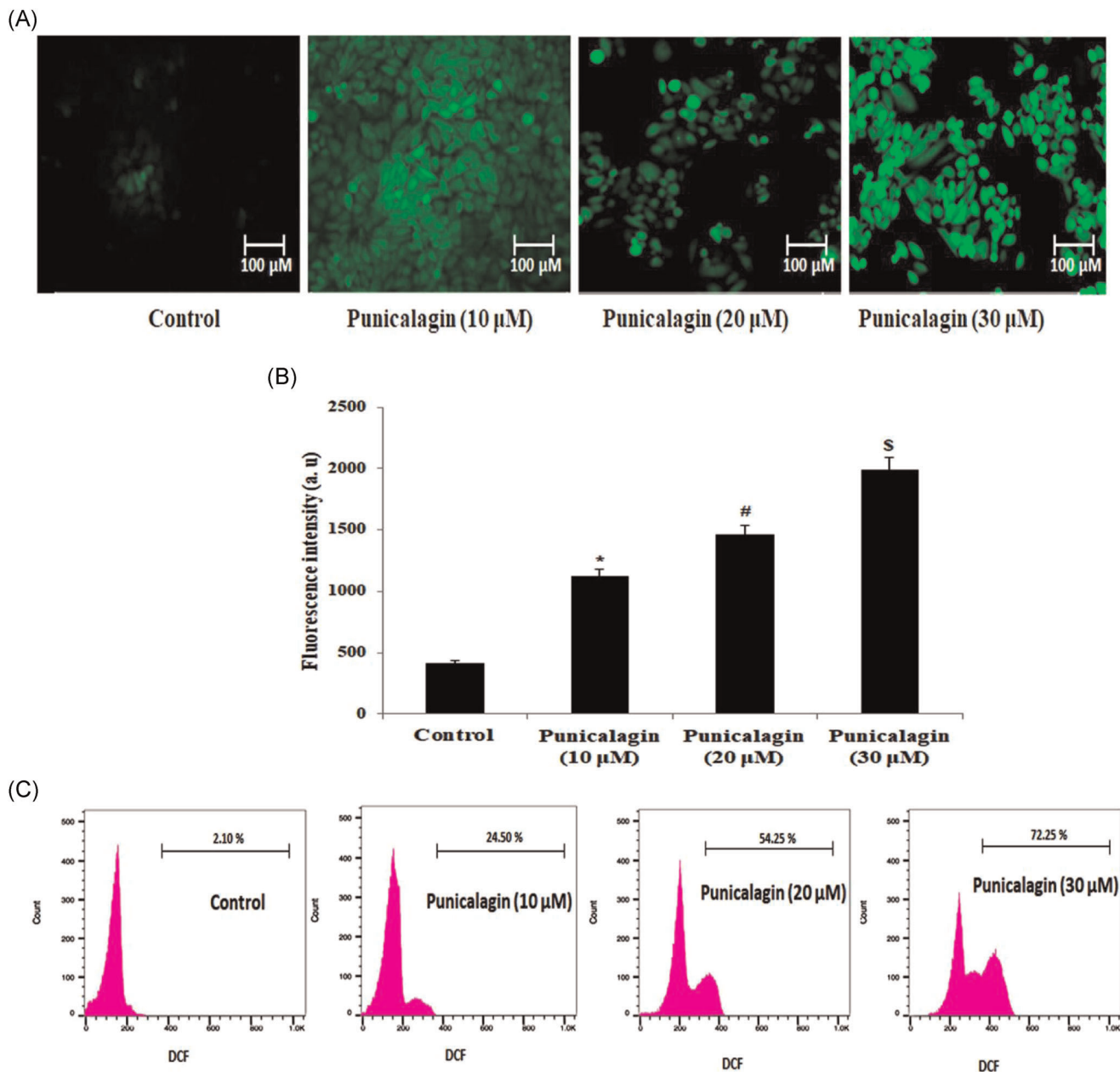


FIGURE 2 Punicalagin produces ROS in A549 cells. (A) Microscopic examination of ROS was tested by DCFH-DA staining and a $\times 20$ microscopic image has been utilized. (B) Bar illustrates the DCFH intensity of A549 cells and was quantified by a fluorometer. All the tests were done in triplicate and all the values were delivered as mean \pm SD. The range of significance was calculated by a one-way ANOVA in the DMRT package. (C) Flow cytometric analysis of punicalagin-induced ROS detection in A549 cells. ANOVA, analysis of variance; DCFH-DA, 2'-7'-dichlorofluorescein diacetate; DMRT, Duncan's multiple range test; ROS, reactive oxygen species

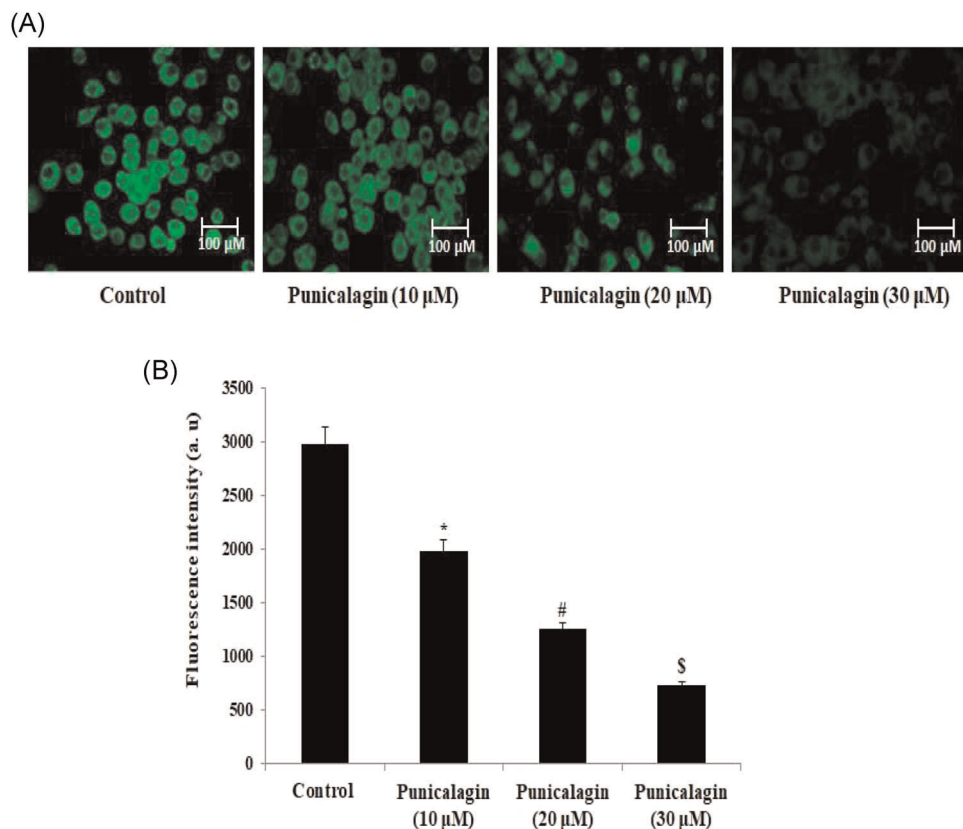


FIGURE 3 Punicalagin alters $\Delta\Psi_m$ in A549 cells. (A) Microscopic examination of $\Delta\Psi_m$ was tested by Rhodamine-123 staining and a $\times 20$ microscopic image has been utilized. (B) Bar illustrates the Rh-123 intensity of A549 cells and was quantified by a fluorometer. All the tests were done in triplicate and all the values were delivered as mean \pm SD. The range of significance was calculated by a one-way ANOVA in the DMRT package. ANOVA, analysis of variance; DMRT, Duncan's multiple range test

allowed high centrifugation (13,000g for 15 min) and the collected samples are considered as a nuclear extract.^[23] The exact protein sample concentration of different groups was estimated by the standard Bradford method. The protein sample was mixed properly with sample buffer and it was separated by the sodium dodecyl sulfate polyacrylamide gel electrophoresis (SDS-PAGE) method, following which the protein was shifted into the nitrocellulose membrane from SDS gel, which was blocked via 5% bovine serum albumin and placed in overnight incubation with specific monoclonal antibodies (STAT-3, IL-6, Bcl-2, JAK-1, Bax, caspase-3, cytochrome-c, and caspase-9) at 4°C. The dilution of the primary monoclonal antibodies was 1:1500. The nitrocellulose membrane were incubated with secondary antibodies with a dilution of 1:5000 for 1 h at 37°C and washed three times by Tris-buffered saline with Tween 20 (TBST) and detected with a chemiluminescence detecting system.

2.9 | Statistical analysis

In this study, SPSS 17 version of the statistical program was used and the data were represented as mean \pm SD. At least three and

maximum of six experiments were done. The data were considered statistically significant at $p < 0.05$.

3 | RESULTS

3.1 | Punicalagin produces toxicity against A549 cells and is nontoxic against HDF cells

Figure 1 showed the punicalagin significantly diminished the cell viability in a concentration-dependent manner. The half maximal inhibitory concentration (IC_{50}) of punicalagin concentration was observed to be 20.5 μ M in A549 cells. Hence, we chose 10, 20, and 30 μ M of punicalagin for further experiment. These findings suggested that punicalagin effectively induced the toxicity associated cell death in A549 cell lines. Table 1 shows the punicalagin-mediated % cell viability in A549 cells. In addition, we demonstrated the punicalagin-mediated cytotoxicity against normal HDF cells (Figure 1B). In this study, we found that punicalagin up to 80 μ M did not cause any toxicity in HDF cells. Moreover, the 90 μ M above concentration of punicalagin significantly exhibits cytotoxicity on HDF cells.

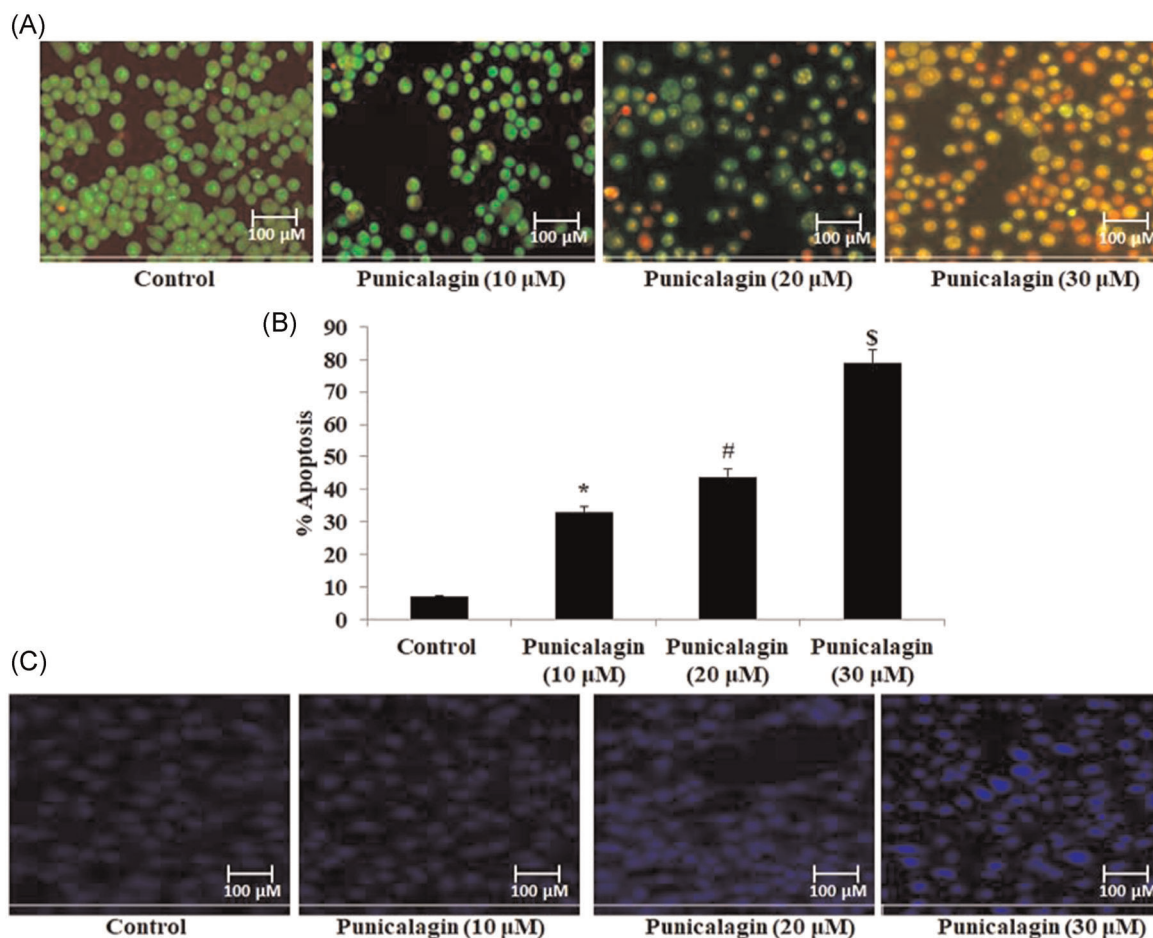


FIGURE 4 Punicalagin-mediated apoptosis signs in A549 cells. (A) AO/EtBr-stained microscopic image illustrated that treated cells show an increased amount of apoptotic cells. (B) Bar diagram represents % apoptosis and data are expressed as mean \pm SD from three independent experiments. $p < 0.05$ is significantly different from the untreated cells. (C) Microscopic image delivered of punicalagin-associated nuclear fragmentation assayed by Hoechst staining. AO/EtBr, acridine orange and ethidium bromide

3.2 | Punicalagin produces ROS in A549 cells

The spectrofluorimetric analysis of ROS production in punicalagin treated cells is seen in Figure 2. A549 cells were added with different concentrations of punicalagin (10, 20, and 30 μM), which showed a high degree of ROS production, which directly corresponds to the enhancement of fluorescence intensity (Figure 2A,B). The A549 cells treated with punicalagin (30 μM) demonstrated higher ROS generation than the punicalagin (10 and 20 μM) treatment. In addition, flow cytometric analysis also confirmed the increased DCF levels observed in A549 cells treated with different concentrations of punicalagin (Figure 2C). These results clearly showed that punicalagin induces ROS in lung cancer cells.

3.3 | Punicalagin alters mitochondrion membrane potential ($\Delta\Psi_m$) in A549 cells

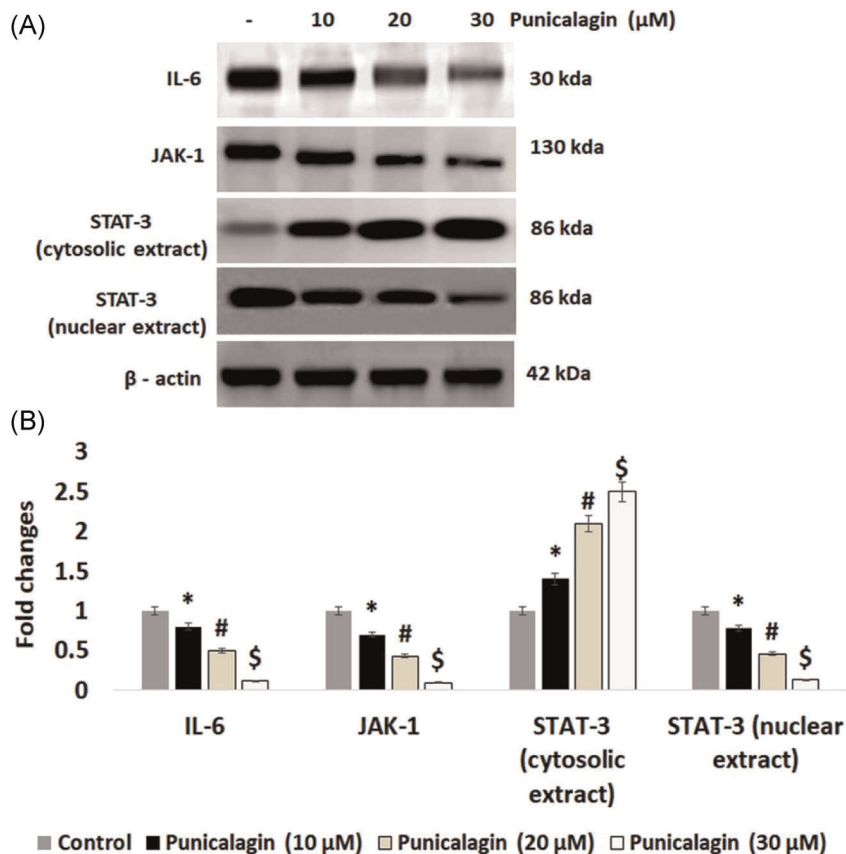
Premature apoptotic activation occurred through the alteration of $\Delta\Psi_m$ and it was evaluated by lipophilic cationic dye Rhodamine-123 staining. As compared with the punicalagin treated cells, the control cells

produced an elevated intensity of green fluorescence that represents a polarized mitochondrial membrane, and it was concluded that there was no alteration of $\Delta\Psi_m$ (Figure 3). Conversely, punicalagin treatment demonstrated a significant alteration of $\Delta\Psi_m$ and showed reduced green fluorescence in A549 cancer cells.

3.4 | Punicalagin-mediated apoptosis signs in A549 cells

The microscopic analysis exhibited the features of the apoptotic hallmarks on punicalagin-treated A549 cells, which were stained with EtBr/AO (Figure 4). The EtBr red colored fluorescence dye penetrated into the condensed nuclei of the apoptotic cells, whereas the AO (green) was uptaken in live cells alone. Hence, our findings illustrated the control cells showed a vast green fluorescence nucleus that represented live cells (Figure 4). Punicalagin (30 μM)-treated cells demonstrated an orange color, indicating the initial form of apoptosis, and also the red colored fragmented nuclei represented late apoptosis. For further confirmation, we performed a Hoechst staining assay to analyze the initiation of

FIGURE 5 Punicalagin inhibits the translocation of STAT-3 in A549 cells. (A) Effect of punicalagin on STAT-3, IL-6, and JAK-1 protein expression by Western blot analysis in A549 cells. The above mentioned protein bands was enumerated by densitometry analysis and an exact protein loading was confirmed by β -actin. (B) The representative graph exhibits the protein expression pattern (STAT-3, IL-6, JAK-1) of fold changes normalized by β -actin. Values from the statistical data are articulated as mean \pm SD for three separate experiments. Values not allocated a marking (*, #, \$) vary significantly at $p < 0.05$ versus control (DMRT). DMRT, Duncan's multiple range test



apoptosis by punicalagin in A549 cancer cells. There, we noticed that 30 μ M of punicalagin treatment effectively causes DNA damage in A549 cells rather than 10 and 20 μ M treatment.

3.5 | Punicalagin inhibits the translocation of STAT-3 in A549 cells

Generally, interleukin-6 and JAK-1 induce the translocation of STAT-3 from the cytosol to the nucleus in the cells. Here, we determined punicalagin inhibits STAT-3 translocation in A549 cells. As Figure 5 exhibits, nontreated A549 cells showed increased upregulation of IL-6 and JAK-1 expressions. The A549 cells were treated with various concentrations of punicalagin (10, 20, and 30 μ M) inhibiting over upregulation of IL-6 and JAK-1 expressions. Moreover, we observed that punicalagin inhibits STAT-3 translocation in A549 cells by observing that punicalagin induces overexpression of cytosolic fraction of STAT-3 and decreased the expression of the nuclear fraction of STAT-3. Here, we found that punicalagin (30 μ M) has more significant activity than punicalagin (10 and 20 μ M).

3.6 | Punicalagin induces apoptotic signaling in A549 cells

We further determined the immunoblotting analysis of punicalagin treatment-induced level of apoptotic gene expression. The different

concentrations of punicalagin treatment (10, 20, and 30 μ M) regulated apoptotic factors in A549 cancer cells (Figure 6). From this investigation, we found that the punicalagin treatment showed more efficient stimulation of proapoptotic proteins such as Bax, cytochrome-c, caspase-9, and caspase-3 in A549 cells. Furthermore, punicalagin treatment-mediated antiapoptotic protein Bcl-2 protein expression was gradually downregulated in A549 cells on a concentration basis.

4 | DISCUSSION

Punicalagin is a polyphenol exhibited in numerous natural products; vegetables and also found in tea and wine.^[24] In this experiment, we focused that the antiproliferative and apoptotic role of punicalagin against lung cancer cells. The antiproliferative and apoptotic impacts of pomegranates have been documented; the source of punicalagin is pomegranate and it has the highest concentrations.^[25] Harmful gliomas are impervious to different expert apoptotic treatments, for example, radiotherapy and regular chemotherapy.^[26] In this present investigation, we analyzed the cytotoxic effect of punicalagin in human A549 cells, by modulating STAT3 flagging and instigating apoptotic cell death. Also, we have observed punicalagin viably upgrades cell death in A549 malignant growth cells. Many earlier anticancer studies have pointed out punicalagin's role in various cell lines. Apoptosis has a crucial function in several biological processes including cell growth, replication, embryonic development,

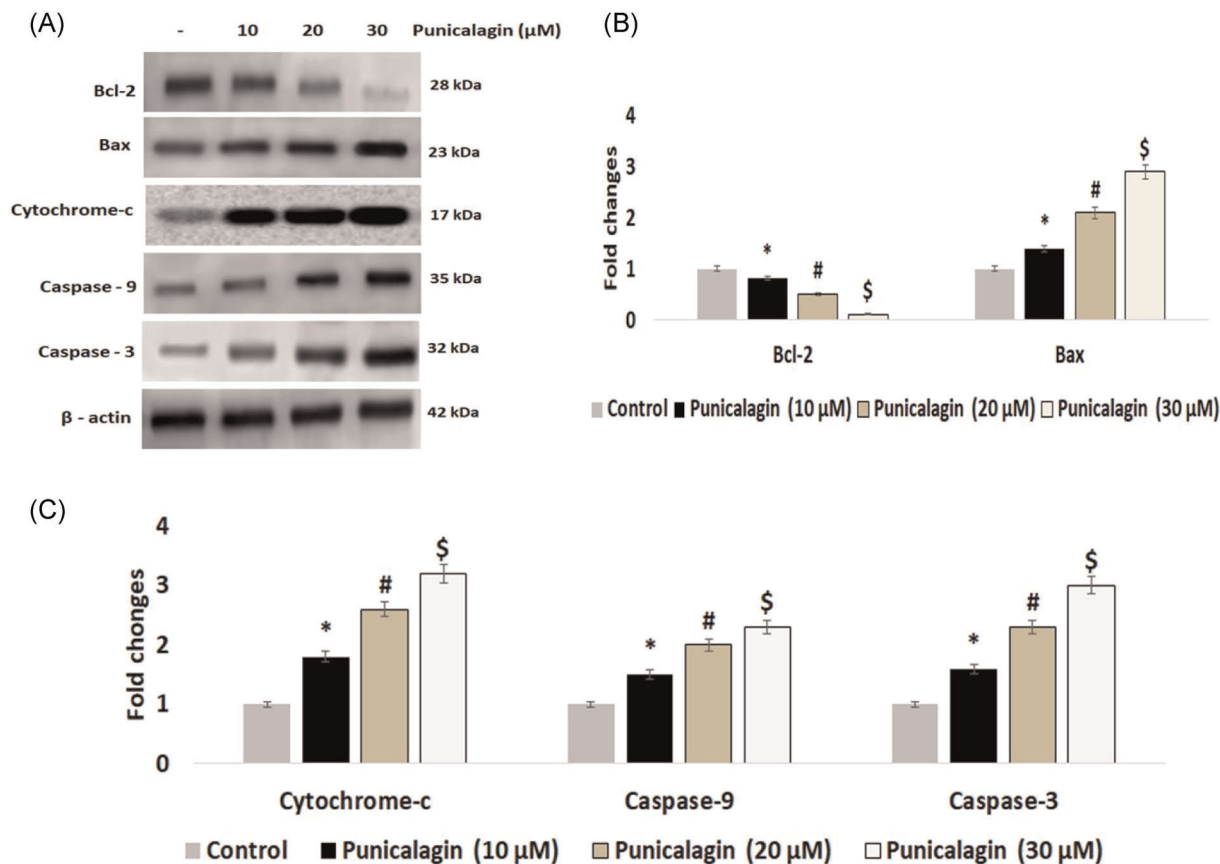


FIGURE 6 Punicalagin induces apoptotic signaling in A549 cells. (A) Effect of punicalagin on apoptotic protein Bax, Bcl-2, caspase-9, cytochrome-c, and caspase-3 by Western blot analysis in A549 cells. The above mentioned protein bands were enumerated by densitometry analysis and an exact protein loading was confirmed by β -actin. (B–C) The representative graph exhibits the protein expression pattern (Bax, Bcl-2, caspase-9, cytochrome-c, and caspase-3) of fold changes normalized by β -actin. Values from the statistical data are articulated as mean \pm SD for three separate experiments. Values not allocated a marking (*, #, \$) vary significantly at $p < 0.05$ versus control (DMRT). DMRT, Duncan's multiple range test

alterations in cell morphology, and chemical-mediated cell death.^[27] It is triggered through various stimuli and enhances ROS level, DNA damage, activation of caspases family, cell contraction, chromatin contraction, and nucleosomal degradation.^[28] Many pieces of evidence have documented that the initiation of apoptosis occurred by the means of reduction of endogenous anti-oxidants depletion or enhanced production of ROS.^[29]

The cells remain alive with lesser ROS levels, but the relative ROS development drives cell cycle arrest or apoptosis. Presently, ROS altering drugs are a radical phenomenon for inventing new treatment strategies to preclude malignant cells.^[30] In this study, punicalagin significantly activated ROS creation in A549 cells; also created mitochondrial brokenness and membrane potential loss, which induced the release of proapoptotic elements. This entered into the cytochrome-c and to the cytosol that finally leads to activate commencement of pro-caspase cascades.^[31]

The excessive generation and accumulation of ROS impair mitochondrial membranes, resulting in a major loss of $\Delta\Psi_m$. This enormous production of ROS and loss of MMP triggers the formation of proapoptotic factors in the cytosolic areas.^[32] In this current

study, we noticed that the punicalagin-induced membrane potential loss and morphological alteration in A549 cells. Also, our findings exposed that the apoptotic cells were found with cell blebbing, shrinkage, and fragmentation of the nucleus, which was confirmed by combinational treatment with the AO/EtBr assay. It has been validated the cell disintegration by showing alive cells were consistent with green fluorescence; early apoptotic cells death was demonstrated in greenish-yellow shaded or green-yellow parts, then the late apoptotic cell death was demonstrated in orange-hued sections. Hence, it was noted that the apoptosis was invigorated either by endogenous cell reinforcements, exhaustion, or expanded production of ROS.^[33] Similarly, we discovered punicalagin incites damage in DNA and thereby a DNA section was seen in A549 cells. Subsequently, our results recommend that punicalagin adequately investigates cell demise in lung malignancy cells. Apoptosis in malignant cells, is the foremost considerable and direct method for controlling the advance of tumor cells.

STAT-3 has a cytoplasmic idle transcriptional factor, which is involved to malignant progression and its inhibition have considered as tumor therapeutic target. Activation of STAT-3 requires

interleukin-mediated phosphorylation of JAK-1 thereby STAT-3 translocate to nucleus and promote carcinogenic signaling.^[34] Hence, the identification of STAT-3-specific inhibitors may be considered as a potential treatment for various cancers, and also many STAT-3 inhibitors are under clinical trials.^[35,36] We also observed punicalagin inhibits IL-6, JAK-1, and STAT-3 activation and thereby induces apoptosis in A549 cells. The translocation ability of STAT-3 was observed by the cytosolic and nuclear fraction of STAT-3 in A549 cells. These results clearly indicated that punicalagin inhibits translocation in a concentration-dependent manner. Previously, caffeic acid has been reported that inhibits translocation of STAT-3 thereby prevents proliferation and angiogenesis in mice models.^[37]

Apoptosis was initiated by several cellular factors that stimulated the modulation of the Bax-Bcl-2 ratio and subsequently induces the expression level of caspases.^[38] The mitochondria-subordinate pathway is the natural pathway that could intermediate between the key apoptotic proteins, including the Bcl-2 family proteins such as, caspase-3 and poly (ADP-ribose) polymerase (PARP).^[39] The Bcl-2 family plays a significant role in the apoptotic process of malignant cells, where it has antiapoptotic protein Terrible and hostile to apoptotic protein of Bcl-2.^[40] Caspase-3 is an important protease in the response and it has been perceived as an objective for malignant growth therapeutics.^[41] This study was done to confirm whether punicalagin-induced apoptosis is mediated by the opening of the mitochondria-dependent pathway or not. By proving this, the results showed that the punicalagin reduced the Bcl-2 protein expression levels and subsequently increased the caspase-3 in a dose-associated manner. In addition, the punicalagin could induce the caspase-3-dependent apoptosis via upregulating Bax and downregulating Bcl-2. Therefore, our study depicted that the punicalagin induces apoptosis in A549 cells via controlling apoptotic pathways. Overall, our investigation explained that punicalagin scavenges ROS-mediated apoptosis in A549 cells. Moreover, punicalagin clearly demonstrated the generation of ROS directly impacted the punicalagin-induced proapoptotic proteins. Punicalagin inhibits IL-6 and JAK-1 and thereby downregulates STAT-3 and its translocation that leads to inactivating Bcl-2 and inducing apoptosis in lung cancer cells.

5 | CONCLUSION

This study found that the punicalagin incites A549 cell apoptosis by an enhanced generation of intracellular ROS production and subsequent altering of the mitochondrion membrane potential to induce proapoptotic markers such as Bax and caspases. Moreover, punicalagin inhibits JAK-1-mediated STAT-3 translocation; thereby inhibiting the antiapoptotic marker of Bcl-2 expression in A549 cells. Thus, punicalagin could be considered as a potential natural drug to promote apoptosis by controlling the JAK-STAT3 flagging pathways.

ACKNOWLEDGMENT

The project was supported by the Natural Science Basic Research Plan in Shaanxi provenance of China (Program No: 2019JQ-993).

CONFLICT OF INTERESTS

The authors declare that there are no conflict of interests.

ORCID

Hong Wang  <http://orcid.org/0000-0002-0740-9218>

Xiaolei Fang  <https://orcid.org/0000-0002-4997-1065>

REFERENCES

- [1] J. E. Larsen, J. D. Minna, *Clin. Chest Med.* **2011**, *32*, 40.
- [2] J. Ferlay, M. Colombet, I. Soerjomataram, C. Mathers, D. M. Parkin, M. Piñeros, A. Znaor, F. Bray, *Int. J. Cancer* **2019**, *144*, 1953.
- [3] T. Goldkorn, S. Filosto, S. Chung, *Antioxid. Redox Signal.* **2014**, *21*, 2174.
- [4] S. Pakkala, S. S. Ramalingam, *JCI Insight* **2018**, *3*, e120858.
- [5] K. Hevener, T. A. Verstak, K. E. Lutat, D. L. Riggsbee, J. W. Mooney, *Acta Pharm. Sin. B* **2018**, *8*, 861.
- [6] G. Y. Liou, P. Storz, *Free Radical Res.* **2010**, *44*, 496.
- [7] A. A. Alfadda, R. M. Sallam, *BioMed. Res. Int.* **2012**, *2012*, 936486.
- [8] D. B. Zorov, M. Juhaszova, S. J. Sollott, *Physiol. Rev.* **2014**, *94*, 950.
- [9] A. Maryam, T. Mehmood, H. Zhang, Y. Li, M. Khan, T. Ma, *Sci. Rep.* **2017**, *7*, 6242.
- [10] J.-h. Ma, L. Qin, X. Li, *Cell Commun. Signal.* **2020**, *18*, 33.
- [11] Y. Shi, Z. Zhang, X. Qu, X. Zhu, L. Zhao, R. Wei, Q. Guo, L. Sun, X. Yin, Y. Zhang, Y. Zhang, X. Li, *Int. J. Oncol.* **2018**, *53*, 7.
- [12] M. Fridlender, Y. Kapulnik, H. Koltai, *Front. Plant Sci.* **2015**, *6*, 799.
- [13] N. Syed, J. C. Chamcheu, M. Adhami, H. Mukhtar, *Anticancer Agents Med. Chem.* **2013**, *13*, 1161.
- [14] P. Sharma, S. F. McClees, F. Afaq, *Molecules* **2017**, *22*, 177.
- [15] S. Bassiri-Jahromi, *Oncol. Rev.* **2018**, *12*, 345.
- [16] F. Mastrogiovanni, A. Mukhopadhyay, N. Lacetera, M. T. Ryan, A. Romani, R. Bernini, *Nutrients* **2019**, *11*, 548.
- [17] J. Li, G. Wang, C. Hou, J. Li, Y. Luo, B. Li, *Food Agric. Immunol.* **2019**, *30*, 898.
- [18] F. Seif, M. Khoshmirsafa, H. Aazami, M. Mohsenzadegan, G. Sedighi, M. Bahar, *Cell Commun. Signal.* **2017**, *15*, 23.
- [19] S. Gunaseelan, A. Balupillai, K. Govindasamy, K. Ramasamy, G. Muthusamy, *PLOS One* **2017**, *12*, e0176699.
- [20] G. Annamalai, S. Kathiresan, N. Kannappan, **2016**, *82*, 236.
- [21] R. Karthikeyan, G. Kanimozhi, N. R. Prasad, B. Agilan, M. Ganesan, G. Srithar, *Life Sci.* **2018**, *212*, 150.
- [22] R. Nilamber Lal Das, S. Muruhan, R. P. Nagarajan, A. Balupillai, *J. Biochem. Mol. Toxicol.* **2019**, *33*, e22263.
- [23] A. Balupillai, R. P. Nagarajan, K. Ramasamy, K. Govindasamy, G. Muthusamy, *Toxicol. Appl. Pharmacol.* **2018**, *352*, 96.
- [24] M. Viuda-Martos, J. Fernández-López, J. A. Pérez-Álvarez, *Compr. Rev. Food Sci. Food Saf.* **2010**, *9*, 654.
- [25] N. P. Seeram, L. S. Adams, S. M. Henning, Y. Niu, Y. Zhang, M. G. Nair, D. Heber, *J. Nutr. Biochem.* **2005**, *6*, 360.
- [26] M. E. Davis, *Clin. J. Oncol. Nurs.* **2016**, *20*, S2.
- [27] S. Elmore, *Toxicol. Pathol.* **2007**, *35*, 516.
- [28] Z. Liu, Z. Ren, J. Zhang, C. C. Huang, E. Kandaswamy, T. Zhou, *Front. Physiol.* **2018**, *9*, 477.
- [29] R. Sabitha, K. Nishi, V. P. Gunasekaran, B. Agilan, E. David, G. Annamalai, R. Vinothkumar, M. Perumal, L. Subbiah, M. Ganesan, *Chem. Biol. Interact.* **2020**, *321*, 109044.
- [30] H. Yang, R. M. Villani, H. Wang, M. J. Simpson, M. S. Roberts, M. Tang, *J. Exp. Clin. Cancer Res.* **2018**, *37*, 266.
- [31] M. Nita, A. Grzybowski, *Oxid. Med. Cell. Longev.* **2016**, *2016*, 3164734.
- [32] U. Muzaffer, V. I. Paul, N. R. Prasad, R. Karthikeyan, *Biochem. Biophys. Rep.* **2018**, *13*, 115.

- [33] D. Hanahan, R. A. Weinberg, *Cell* **2011**, *144*, 674.
- [34] D. E. Johnson, R. A. O'Keefe, J. R. Grandis, *Nat. Rev. Clin. Oncol.* **2018**, *15*, 234.
- [35] F. Laudisi, F. Cherubini, G. Monteleone, C. Stolfi, *Int. J. Mol. Sci.* **2018**, *19*, 1787.
- [36] J. J. Qin, L. Yan, J. Zhang, W. D. Zhang, *J. Exp. Clin. Cancer Res.* **2019**, *38*, 195.
- [37] B. Agilan, N. Rajendra Prasad, G. Kanimozhi, R. Karthikeyan, M. Ganesan, S. Mohana, *Photochem. Photobiol.* **2016**, *92*, 474.
- [38] M. Mancini, D. W. Nicholson, S. Roy, N. A. Thornberry, E. P. Peterson, L. A. Casciola-Rosen, *J. Cell. Biol.* **1988**, *140*, 1495.
- [39] M. K. Sharief, M. Douglas, M. Noori, Y. K. Semra, *J. Neuroimmunol.* **2002**, *125*, 162.
- [40] R. Gerl, D. L. Vaux, *Carcinogenesis* **2005**, *26*, 270.
- [41] S. H. MacKenzie, A. C. Clark, *Curr. Cancer Drug. Targets* **2008**, *8*, 98.

How to cite this article: L. Fang, H. Wang, J. Zhang, X. Fang, *J Biochem Mol Toxicol.* **2021**, e22771.

<https://doi.org/10.1002/jbt.22771>